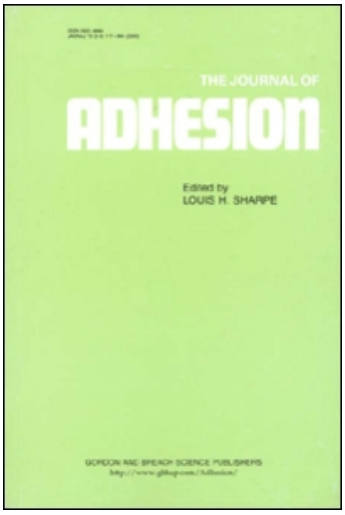

The Journal of Adhesion
Publication details, including instructions for authors and subscription information:
http://www.informaworld.com/smpp/title~content=t713453635

Two-Dimensional Transient Thermal Stress Analysis of Adhesive Butt Joints

Masahide Katsuo[a]; Yuichi Nakano[a]; Toshiyuki Sawa[b]
[a] Depart ent of Mechanical Engineering, Shonan Institute of Technology, Fujisawa, Japan [b] Depart ent of Mechanical Engineering, Ya anashi University, Takeda, Kofu, Japan

To cite this Article Katsuo, Masahide , Nakano, Yuichi and Sawa, Toshiyuki(1999) 'Two-Dimensional Transient Thermal Stress Analysis of Adhesive Butt Joints', The Journal of Adhesion, 70: 1, 75 — 93
To link to this Article: DOI: 10.1080/00218469908010488
URL: http://dx.doi.org/10.1080/00218469908010488

J. Adhesion, 1999, Vol. 70, pp. 75–93
Reprints available directly from the publisher
Photocopying permitted by license only

Two-Dimensional Transient Thermal Stress Analysis of Adhesive Butt Joints

MASAHIDE KATSUO[a,*], YUICHI NAKANO[a] and TOSHIYUKI SAWA[b]

[a]*Department of Mechanical Engineering, Shonan Institute of Technology, 1-1-25 Nishikaigan Tsujido, Fujisawa 251, Japan;*
[b]*Department of Mechanical Engineering, Yamanashi University, 4-3-11 Takeda, Kofu 400, Japan*

(Received 20 August 1998; In final form 7 January 1999)

Transient thermal stress distribution in an adhesive butt joint is considered. It is assumed that both the upper and lower end surfaces of the joint are maintained at different temperatures at a certain instant in time and that no heat transfers between the side surfaces of the joint and ambient air. In the analysis, two adherends were replaced with finite strips and unsteady temperature distribution in the joint was obtained theoretically. Then the transient thermal stress distribution in the joint was analyzed using a two-dimensional theory of elasticity. The effects of the ratios of the coefficient of thermal expansion and Young's modulus of the adherend to those of the adhesive on the thermal stress distribution were clarified from numerical calculations. Furthermore, the transient stress distribution in the adhesive was measured by a photoelastic experiment on a joint where the adhesive was modelled by an epoxy plate. The experimental results were consistent with the analytical results.

Keywords: Transient thermal stress; theory of elasticity; thermoelastic potential; photoelasticity

1. INTRODUCTION

Adhesive joints are now widely used in engineering structures because they have several attractive features. These include the ease by which different materials are joined; lightened joined structure; and uniform stress distribution, especially when compared with conventional bolted, riveted and welded joints.

*Corresponding author. Tel.: 81-466-34-4111, Ext. 635, Fax: 81-466-34-9527.

Electronic devices are composed of different kinds of small components and a substrate and they are mostly joined by soldering or adhesive bonding. In electronic devices, mechanical and thermal properties of the component materials and an adhesive bond, such as Young's modulus, Poisson ratio, the coefficient of thermal expansion and the thermal conductivity, are generally quite different from each other. Therefore, thermal stresses are generated easily in the device when it is under some temperature distribution and they may cause a failure or a fracture of the device even if it is free from any mechanical loading. Some analytical work [1–3] has been carried out on the thermal stresses in electronic devices or in adhesive joints subjected to temperature changes. However, these are mostly in the case of a steady-state temperature and the analytical [4] and experimental [5, 6] studies concerning transient thermal stresses and strength are few.

The aim of this study is to clarify transient behavior of the thermal stress in an adhesive butt joint when both the upper and lower surfaces of the joint are heated suddenly, at a certain point in time, by a surrounding fluid, after bonding and curing at a uniform temperature. In the analysis, unsteady one-dimensional temperature distribution in the joint is examined using the Laplace transform and the residue theorem, and then the transient thermal stress distribution is analyzed using a two-dimensional theory of elasticity. The effects of mechanical and thermal properties of the joint on the transient thermal stress distributions at the interface between the adherends and the adhesive are clarified by numerical calculations. In addition, photoelastic experiments were carried out in which an epoxy resin plate was modelled as the adhesive and the numerical results were compared with the experimental ones.

2. THEORETICAL ANALYSIS

Figure 1 shows an analytical model of an adhesive butt joint where two adherends are joined by an adhesive at uniform temperature. In the analysis, the following thermal conditions are assumed: initially the joint is kept at 0°C, and both the upper and lower surfaces of the joint are heated suddenly by surrounding with fluid of temperatures T_u and T_l, respectively, while the side surfaces of the joint are insulated.

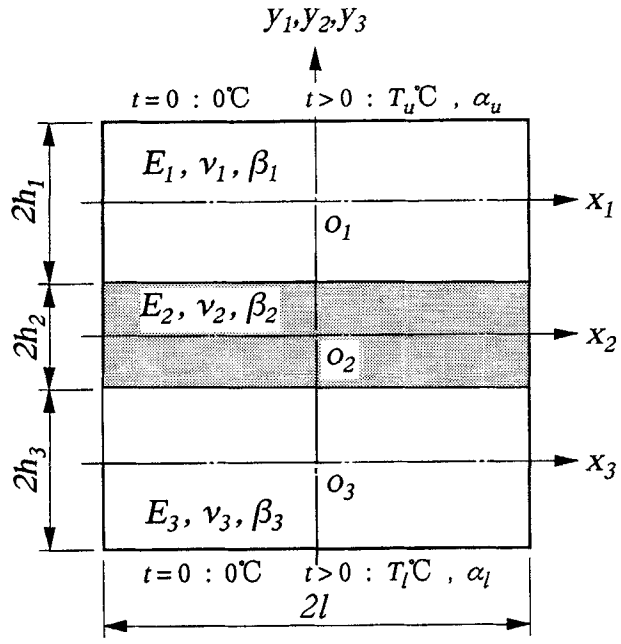

FIGURE 1 Analytical model of adhesive butt joint.

Heat transfer coefficients between the upper and lower surfaces of the joint and surrounding fluid are denoted as α_u and α_l, respectively. Two adherends and the adhesive are replaced with finite strips 1, 2 and 3. The thickness and the width of each finite strip are denoted by $2h_i$ ($i = 1, 2$ and 3) and $2l$, respectively. In the figure, x_i and y_i axes are adopted as the coordinates and the origins O_1, O_2 and O_3 are fixed at the center of each finite strip. The Young's modulus, Poisson's ratio and the coefficient of thermal expansion of each finite strip are denoted by E_i, ν_i and β_i, respectively, and these material properties are assumed to be constant and independent of temperature.

2.1. Temperature Distribution

In the first step of the thermal stress analysis, the temperature distributions in each finite strip should be obtained. For the joint model

shown in Figure 1, there is no temperature change in the thickness, z-direction, of the joint so that the analysis can be simplified by treating the heat conduction problem as a one-dimensional problem governed by the coordinate y_i since the side surfaces of the joint are insulated. Thus, the fundamental equation for one-dimensional transient heat transfer is simply expressed as Eq. (1), where the transient temperature distribution in each finite strip is denoted by $T_i^t(y_i, t)$, $i = 1, 2$ and 3 [7].

$$\frac{\partial T_i^t(y_i, t)}{\partial t} = a_i \frac{\partial^2 T_i^t(y_i, t)}{\partial y_i^2} \tag{1}$$

where, t: time, a: thermal diffusivity ($= K/\varrho c$), K: thermal conductivity, ϱ: density and c: specific heat.

The initial and thermal boundary conditions of the joint are expressed as the following Eqs. (2) and (3), respectively.

$$T_1^t(y_1, 0) = T_2^t(y_2, 0) = T_3^t(y_3, 0) = 0 \tag{2}$$

$$\left.\begin{aligned}
&K_1 \frac{\partial T_1^t(h_1, t)}{\partial y_1} = \alpha_u \{T_u - T_1^t(h_1, t)\} \\
&T_1^t(-h_1, t) = T_2^t(h_2, t) \\
&K_1 \frac{\partial T_1^t(-h_1, t)}{\partial y_1} = K_2 \frac{\partial T_2^t(h_2, t)}{\partial y_2} \\
&T_2^t(-h_2, t) = T_3^t(h_3, t) \\
&K_2 \frac{\partial T_2^t(-h_2, t)}{\partial y_2} = K_3 \frac{\partial T_3^t(h_3, t)}{\partial y_3} \\
&K_3 \frac{\partial T_3^t(h_3, t)}{\partial y_3} = \alpha_l \{T_3^t(h_3, t) - T_l\}
\end{aligned}\right\} \tag{3}$$

Using the Laplace transform of the temperature distribution, $T_i^t(y_i, t)$, the transformed transient temperature distributions, $T_i^*(y_i, \omega)$, in each finite strip governed by Eq. (1) can be expressed as the following Eq. (4) [4] taking account of the initial condition of Eq. (2).

$$T_i^*(y_i, \omega) = A_i^* \cos(\gamma_i \omega y_i) + B_i^* \sin(\gamma_i \omega y_i) \tag{4}$$

where $L\{T_i^t(y_i, t)\} = T_i^*(y_i, \omega)$, $\omega^2 = -s$ (s: *Laplace parameter*), $\gamma_i^2 = 1/a_i$, $i = 1, 2, 3$.

A_i^* and B_i^* are the unknown coefficients, which should be determined so as to satisfy the boundary conditions of Eq. (3). By substituting Eq. (4) into the Laplace-transformed boundary conditions, these equations are written as the following matrix form:

$$[a_{kl}]\{A_1^*, B_1^*, A_2^*, B_2^*, A_3^*, B_3^*\}^T = \frac{1}{s}\{c_k\} \quad (k, l = 1 \sim 6) \tag{5}$$

where, $[a_{kl}]$ is the coefficient matrix, a superscript T designates the transposition of the vector and $\{c_k\}$ is the constant vector.

Using Cramer's formula, A_i^* and B_i^* can be determined from Eq. (5) and the temperature distributions in the transformed domain are expressed as Eq. (6).

$$T_i^*(y_i, \omega) = \frac{\overline{A_i^*}(\omega)\cos(\gamma_i \omega y_i) + \overline{B_i^*}(\omega)\sin(\gamma_i \omega y_i)}{s\Delta(\omega)}$$
$$\Delta(\omega) = |a_{kl}| = \det[a_{kl}] \tag{6}$$

In this equation, $\Delta(\omega)$ is the determinant of the coefficient matrix $[a_{kl}]$ and the coefficients $\bar{A}_i^*(\omega)$ and $\bar{B}_i^*(\omega)$ are defined as the determinant of the matrix in which the $(2i-1)$-th column and $2i$-th column in the matrix $[a_{kl}]$ are each replaced by the constant vector $\{c_k\}$.

Finally, using the residue theorem, the transient temperature distributions in the domain of time are given by the summation of the residue as the following Eq. (7).

$$T_i'(y_i, t) = \sum_{j=1}^{\infty} \frac{2\exp(-\omega_j^2 t)}{\omega_j \Delta'(\omega_j)} [\overline{A_i^*}(\omega_j)\cos(\gamma_i \omega_j y_i) + \overline{B_i^*}(\omega_j)\sin(\gamma_i \omega_j y_i)] \tag{7}$$

where ω_j represents the j-th positive roots of $\Delta(\omega) = 0$ $(j = 1, 2, 3, \ldots)$ and $\Delta'(\omega)$ is defined as the partial derivative of $\Delta(\omega)$ with respect to ω and expressed as Eq. (8).

$$\Delta'(\omega_j) = \left.\frac{d\Delta(\omega)}{d\omega}\right|_{\omega \to \omega_j} \tag{8}$$

Secondly, the fundamental equation for the steady temperature distribution, $T_i^s(y_i)$, is expressed as the following Eq. (9) and the thermal boundary conditions are expressed similarly as Eq. (3).

$$\frac{\partial^2 T_i^s(y_i)}{\partial y_i^2} = 0 \quad (i = 1, 2 \text{ and } 3) \tag{9}$$

From the solution of Eq. (9), the steady temperature, $T_i^s(y_i)$, is written as the following from taking account of the initial condition of Eq. (2).

$$T_i^s(y_i) = A_i^s + B_i^s y_i \tag{10}$$

where A_i^s and B_i^s are the unknown coefficients determined similarly so as to satisfy the above boundary conditions of Eq. (3). Finally, the temperature distribution in the joint is obtained by adding the transient component expressed in Eq. (7) to the steady component expressed in Eq. (10).

2.2. Thermal Stress

In order to analyze the thermal stress distribution in the joint, thermoelastic potentials $\Omega^t(y_i, t)$ and $\Omega^s(y_i)$, obtained from the respective transient and steady temperatures as shown in Eq. (11), are adopted in this study. The potentials $\Omega^t(y_i, t)$ and $\Omega^s(y_i)$ can be expressed as Eq. (12) from Eqs. (7) and (10), respectively.

$$\left.\begin{aligned} \nabla^2 \Omega_i^t(y_i, t) &= T_i^t(y_i, t) \\ \nabla^2 \Omega_i^s(y_i) &= T_i^s(y_i) \end{aligned}\right\} \tag{11}$$

$$\left.\begin{aligned} \Omega_i^t(y_i, t) &= \sum_{j=1}^{\infty} \frac{-2\exp(-\omega_j^2 t)}{\gamma_i^2 \omega_j^3 \Delta'(\omega_j)} [\overline{A_i^*} \cos(\gamma_i \omega_j y_i) + \overline{B_i^*} \sin(\gamma_i \omega_j y_i)] \\ \Omega_i^s(y_i) &= A_i^s \frac{y_i^2}{2} + B_i^s \frac{y_i^3}{6} \end{aligned}\right\} \tag{12}$$

The thermal stresses and the displacements obtained from the thermoelastic potential, Ω, are expressed as Eq. (13) using a subscript o.

$$\left.\begin{aligned} &\sigma_{xo} = -E\beta\frac{\partial^2\Omega}{\partial y^2},\ \sigma_{yo} = -E\beta\frac{\partial^2\Omega}{\partial x^2},\ \tau_{xyo} = E\beta\frac{\partial^2\Omega}{\partial x\partial y} \\ &2Gu_{xo} = E\beta\frac{\partial\Omega}{\partial x},\ 2Gv_{yo} = E\beta\frac{\partial\Omega}{\partial y} \end{aligned}\right\} \tag{13}$$

where G is the shear modulus.

In practice, however, the boundary conditions with regard to the stresses and the displacements in the joint, which are expressed as Eq. (14), are not always satisfied by only the thermoelastic potential, Ω.

$$\left.\begin{aligned} &\text{At the side surfaces of the joint,} \\ &\qquad x = \pm l : \sigma_{x1} = \sigma_{x2} = \sigma_{x3} = \tau_{xy1} = \tau_{xy2} = \tau_{xy3} = 0 \\ &\text{Both upper and lower surfaces of the joint,} \\ &\quad y = +h_1 : \sigma_{y1} = \tau_{xy1} = 0,\ y = -h_3 : \sigma_{y3} = \tau_{xy3} = 0 \\ &\text{and at the interfaces between the adhesive and the adherends,} \\ &\quad y = -h_1,\ +h_2 : \sigma_{y1} = \sigma_{y2},\ \tau_{xy1} = \tau_{xy2},\ u_{x1} = u_{x2},\ \frac{\partial v_{y1}}{\partial x} = \frac{\partial v_{y2}}{\partial x} \\ &y = -h_2,\ +h_3 : \sigma_{y2} = \sigma_{y3},\ \tau_{xy2} = \tau_{xy3},\ u_{x2} = u_{x3},\ \frac{\partial v_{y2}}{\partial x} = \frac{\partial v_{y3}}{\partial x} \end{aligned}\right\} \tag{14}$$

In order to satisfy these boundary conditions completely, the thermal stress distributions and the displacements in the joint are analyzed using the Airy stress function, $\chi(x, y)$, which must satisfy the biharmonic equation (15).

$$\nabla^2\nabla^2\chi(x,\ y) = 0 \tag{15}$$

The stresses and the displacements obtained from $\chi(x, y)$ are expressed as the following Eq. (16) using a subscript a:

$$\left.\begin{aligned} &\sigma_{xa} = \frac{\partial^2\chi}{\partial y^2},\ \sigma_{ya} = \frac{\partial^2\chi}{\partial x^2},\ \tau_{xya} = -\frac{\partial^2\chi}{\partial x\partial y} \\ &2Gu_{xa} = -\frac{\partial\chi}{\partial x} + \frac{1}{1+\nu}\frac{\partial\phi}{\partial y},\ 2Gv_{ya} = -\frac{\partial\chi}{\partial y} + \frac{1}{1+\nu}\frac{\partial\phi}{\partial x} \\ &\text{where, } \nabla^2\chi = \frac{\partial^2\phi}{\partial x\partial y}. \end{aligned}\right\} \tag{16}$$

The Airy stress function, $\chi(x, y)$, which is suitable for the present joint model, is chosen from the solutions of Eq. (15) in consideration of Eqs. (13) and (14) and expressed as follows [3]:

$$\chi(x, y) = \chi_0 + \chi_1 + \chi_2 + \chi_3 + \chi_4 \tag{17}$$

where, $\chi_0 = \frac{A_0}{2}y^2 + \frac{B_0}{2}x^2$

$$\chi_1 = \sum_{n=1}^{\infty} \frac{\bar{A}_n}{\bar{\Delta}_n \alpha_n^2} [\{\sinh(\alpha_n l) + \alpha_n l \cosh(\alpha_n l)\} \cosh(\alpha_n x) - \sinh(\alpha_n l)\, \alpha_n x \sinh(\alpha_n x)] \cos(\alpha_n y) + \sum_{s=1}^{\infty} \frac{\bar{B}_s}{\bar{\Omega}_s \lambda_s^2} [\{\sinh(\lambda_s h) + \lambda_s h \cosh(\lambda_s h)\} \cosh(\lambda_s y) - \sinh(\lambda_s h)\, \lambda_s y \sinh(\lambda_s y)] \cos(\lambda_s x)$$

$$\chi_2 = \sum_{n=1}^{\infty} \frac{\bar{\bar{A}}_n}{\bar{\bar{\Delta}}_n \alpha_n'^2} [\{\sinh(\alpha_n' l) + \alpha_n' l \cosh(\alpha_n' l)\} \cosh(\alpha_n' x) - \sinh(\alpha_n' l)\, \alpha_n' x \sinh(\alpha_n' x)] \sin(\alpha_n' y) + \sum_{s=1}^{\infty} \frac{\bar{\bar{B}}_s}{\bar{\bar{\Omega}}_s \lambda_s^2} [\{\cosh(\lambda_s h) + \lambda_s h \sinh(\lambda_s h)\} \sinh(\lambda_s y) - \cosh(\lambda_s h)\, \lambda_s y \cosh(\lambda_s y)] \cos(\lambda_s x)$$

$$\chi_3 = \sum_{n=1}^{\infty} \frac{\bar{A}_n'}{\bar{\Delta}_n' \alpha_n'^2} \{\cosh(\alpha_n' l)\, \alpha_n' x \sinh(\alpha_n' x) - \alpha_n' l \sinh(\alpha_n' l) \cosh(\alpha_n' x)\} \cos(\alpha_n' y) + \sum_{s=1}^{\infty} \frac{\bar{B}_s'}{\bar{\Omega}_s' \lambda_s'^2} \{\cosh(\lambda_s' h) \lambda_s' y \sinh(\lambda_s' y) - \lambda_s' h \sinh(\lambda_s' h) \cosh(\lambda_s' y)\} \cos(\lambda_s' x)$$

$$\chi_4 = \sum_{n=1}^{\infty} \frac{\bar{\bar{A}}_n'}{\bar{\bar{\Delta}}_n' \alpha_n^2} \{\cosh(\alpha_n l)\, \alpha_n x \sinh(\alpha_n x) - \alpha_n l \sinh(\alpha_n l) \cosh(\alpha_n x)\} \sin(\alpha_n y) + \sum_{s=1}^{\infty} \frac{\bar{\bar{B}}_s'}{\bar{\bar{\Omega}}_s' \lambda_s'^2} \{\sinh(\lambda_s' h)\, \lambda_s' y \cosh(\lambda_s' y) - \lambda_s' h \cosh(\lambda_s' h) \sinh(\lambda_s' y)\} \cos(\lambda_s' x)$$

and $\alpha_n = \frac{n\pi}{h}$, $\alpha_n' = \frac{(2n-1)\pi}{2h}$, $\lambda_s = \frac{s\pi}{l}$,

$\lambda_s' = \frac{(2s-1)\pi}{2l}$ $(n, s = 1, 2, 3, \ldots)$.

In Eq. (17), A_0, B_0, $\bar{A}_n$, $\bar{B}_s, \ldots, \bar{\bar{A}}_n'$, $\bar{\bar{B}}_s'$ $(n = s = 1, 2, 3, \ldots)$ are unknown coefficients. The thermal stresses and the displacements in the

joint are calculated by superposing each component of the stresses and the displacements obtained from the thermoelastic potential, Ω, on those obtained from the Airy stress function, $\chi(x, y)$, and by substituting the obtained values into the boundary conditions of Eq. (14), the infinite simultaneous equations with these unknown coefficients are derived. Then the coefficients can be determined by solving the simultaneous equations numerically and, finally, the thermal stresses and the displacements of each strip can be calculated.

3. EXPERIMENTAL METHOD

In photoelastic experiments, an epoxy resin plate, the width, the height and the thickness of which were 80, 20 and 6 mm, respectively, was used as an adhesive in the joint. The epoxy resin plate was placed between the upper and lower adherends and was bonded to each of them at a constant temperature (30°C) by an epoxy adhesive (Cemedine Co., EP128), the mechanical properties of which were similar to those of the epoxy resin plate. Afterwards, both the upper and lower surfaces of the joint were cooled instantaneously by surrounding with cold water or only the lower surface was cooled and the upper one was surrounded by air, while the side surfaces of the joint were covered with heat-insulating material. Figure 2 shows the experimental setup, and the shaded area in the figure indicates the cross section of an acrylic resin water tank.

An isochromatic fringe pattern produced on the epoxy resin plate was observed by photoelasticity and photographed at various intervals. Two models of the adhesive butt joint were examined; one was made of steel plates and the other of copper plates as the adherends. Table I lists the material properties of the adherend plates and the adhesive used in the experiment.

4. ANALYTICAL RESULTS AND COMPARISONS WITH EXPERIMENTAL RESULTS

In order to estimate the thermal strength of an adhesive butt joint subjected to the transient temperature changes, the thermal stress

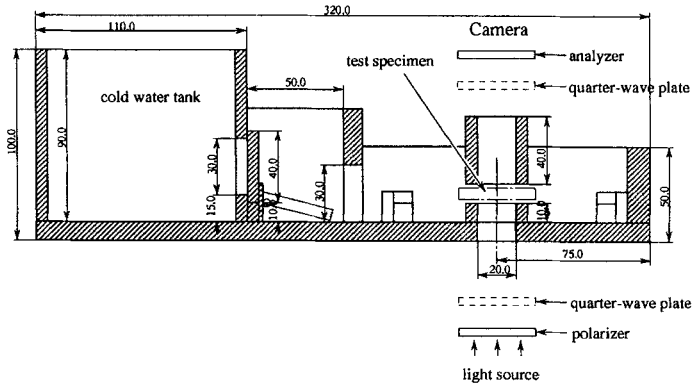

FIGURE 2 Experimental setup (dimensions in mm).

TABLE I Properties of the materials in the joints used in the experiments

	Steel	*Copper*	*Epoxy*
Thermal conductivity K, W/(m K)	54.0	380	0.3
Density ρ, kg/m^3	7830	8900	1400
Specific heat c, J/(kg K)	460	410	1500
Thermal expansion coef. β, (1/K)	11E−6	16.5E−6	60E−6
Young's modulus E, GPa	206	125	3.4
Poisson ratio ν	0.3	0.4	0.38

distributions at the interface between an adherend and an adhesive are examined numerically.

In numerical computations of the transient component of the temperature distribution, the thermoelastic potential and the Airy stress function, shown in Eqs. (7), (12) and (17), respectively, the number of terms of the infinite series is taken as 100 so that a satisfactory degree of convergence is expected.

4.1. Numerical Results

Figure 3 shows the transient temperature variation with respect to the dimensionless time, Fourier number F_r, which is defined as $a_1 t/h_0^2$ and h_0 is the total height of the joint ($=2h_1+2h_2+2h_3$) in this analysis, when both the upper and lower surfaces of the joint in which the

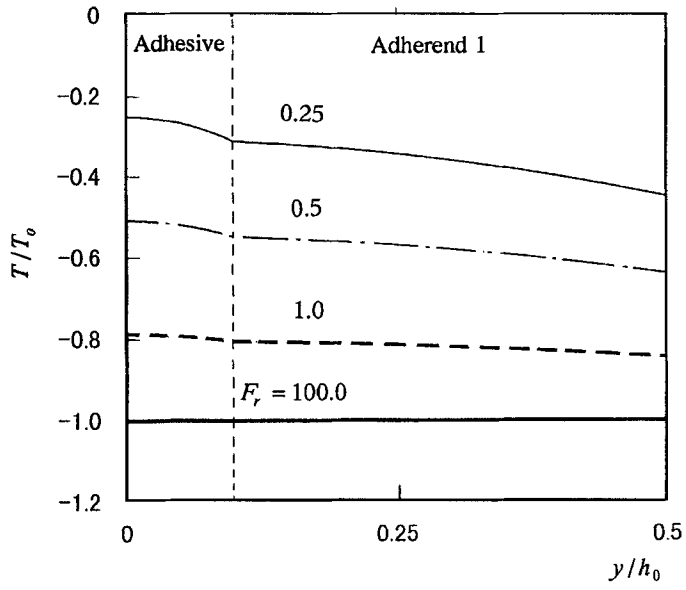

FIGURE 3 Transient temperature distribution in the y-direction ($T_u = T_l = -10°C$, $h_1/h_2 = 2$, $E_1/E_2 = 100$, $\beta_2/\beta_1 = 100$, $K_1/K_2 = 10$).

adherends are made of the same material are cooled instantaneously by surrounding fluid of the same temperature $T_u = T_l = T_0 = -10°C$. In the figure, the ordinate indicates the temperature variation which is normalized by T_0 and the abscissa the position in the y-direction also normalized by h_0. In this case, since the temperature distribution is symmetrical with respect to the x_2 axis where the origin is fixed at the center of the adhesive, the temperature variation in the upper half of the joint is shown in the figure. It is seen that the gradient of the temperature distribution in the adhesive is larger since its thermal conductivity is smaller than that of the adherends, and the temperature becomes uniform in the joint after passage of a long time. The joint was considered to be at a steady temperature state when the dimensionless time $F_r = 100$.

Figures 4(a), 4(b) and 4(c) show the normal, σ_y, σ_x and the shear, τ_{xy}, thermal stress variations which are normalized by $(E_1 \beta_1 T_0)$, at the interface between the adherend and the adhesive, respectively. The abscissa in the figures is also normalized by half the width, l, of the

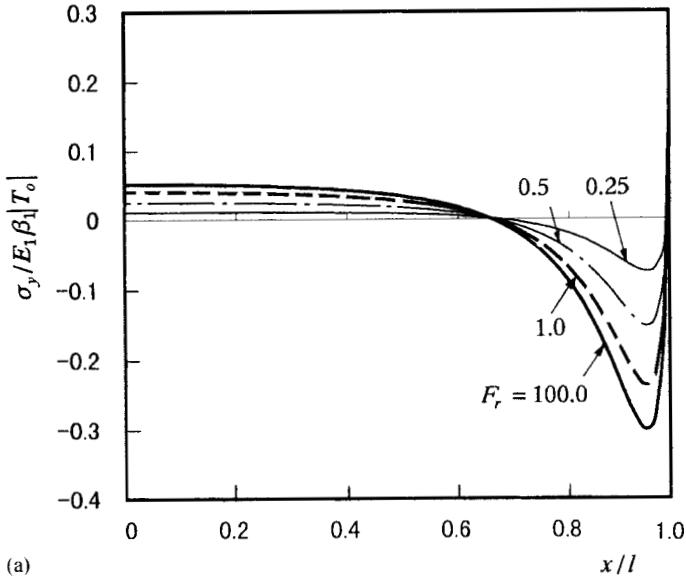

(a)

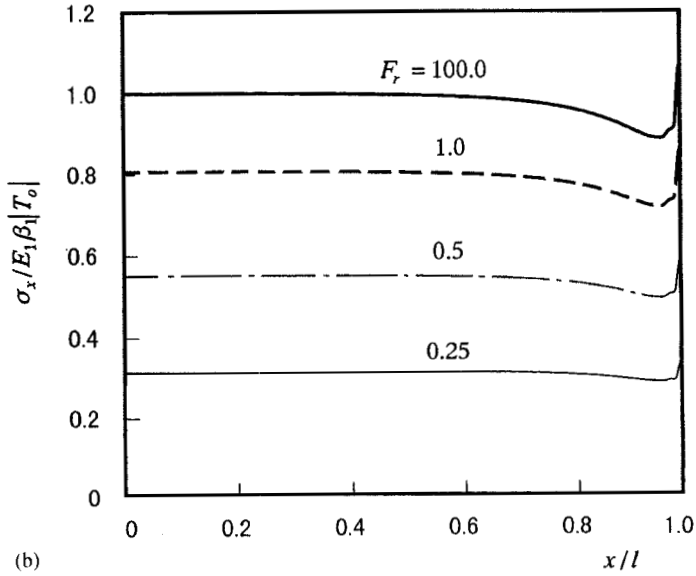

(b)

FIGURE 4 Transient thermal stress distributions at the interface ($T_u = T_l = -10°C$, $h_1/h_2 = 2$, $E_1/E_2 = 100$, $\beta_2/\beta_1 = 100$, $K_1/K_2 = 10$). (a) Normal stress distribution, σ_y; (b) Normal stress distribution, σ_x; (c) Shear stress distribution, τ_{xy}.

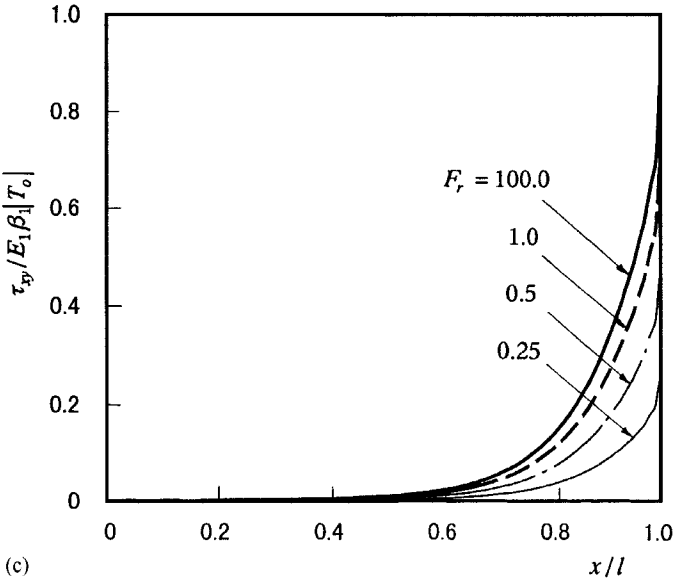

FIGURE 4 (Continued).

joint. From the figures, the normalized transient thermal stress, σ_y, becomes compressive near the ends of the interface between the adhesive and the adherend, while it is tensile in its middle section. However, it changes to tensile and becomes singular at the ends of the interface. The thermal stress, σ_x, increases uniformly with an increase of the dimensionless time throughout the interface; however, in contrast, the thermal stresses, σ_y and τ_{xy}, increase rapidly near the ends of the interface with a short passage of the dimensionless time. The stresses σ_x and τ_{xy} decrease rapidly approaching the edges of the interface and they become 0 at the exact edge ($x = \pm l$) at any time. On the other hand, the stress σ_y shows a stress singularity at the edges of the interface.

Figure 5 shows the transient temperature variation when the lower surface of the joint is cooled instantaneously by the surrounding fluid at $-10°C$, while the upper one is surrounded by air at $0°C$ ($T_u = 0°C$, $T_l = T_0 = -10°C$) and in Figure 6, the normalized thermal stress distribution, σ_y, at the interface between the adhesive and the lower adherend is shown. It is seen from the figure that the value of the

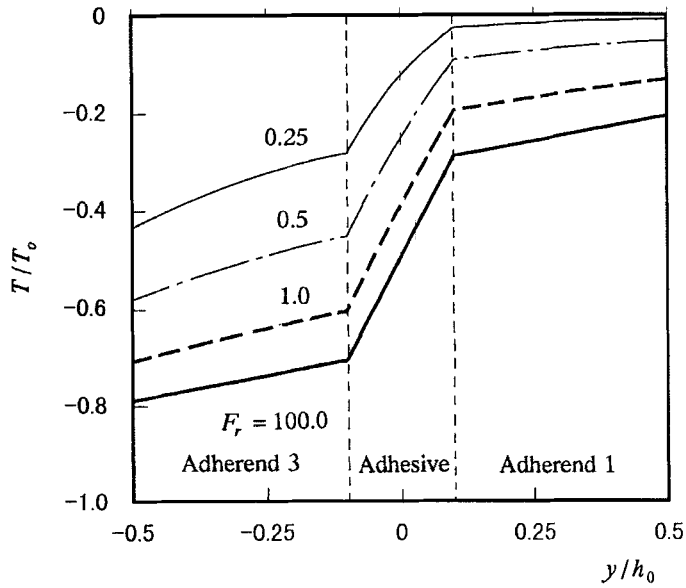

FIGURE 5 Transient temperature variation in the y-direction of the joint ($T_u = 0°C$, $T_l = -10°C$, $h_1/h_2 = 2$, $E_1/E_2 = 100$, $\beta_2/\beta_1 = 100$, $K_1/K_2 = 10$).

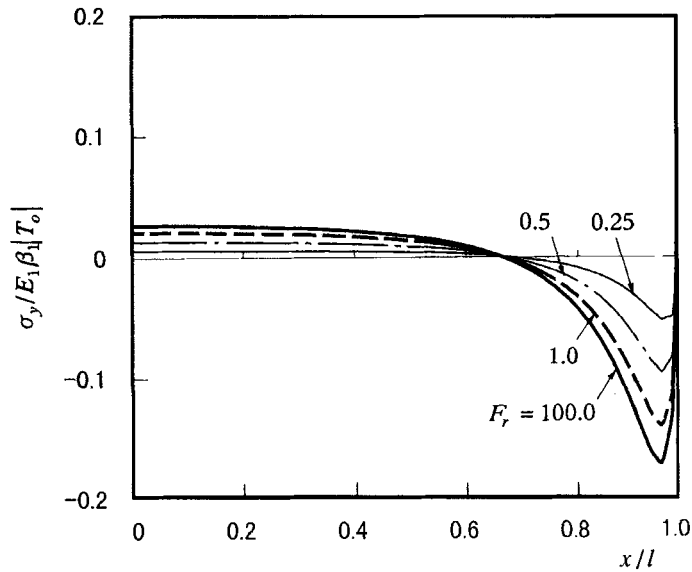

FIGURE 6 Transient thermal stress distribution, σ_y, at the lower interface ($T_u = 0°C$, $T_l = -10°C$, $h_1/h_2 = 2$, $E_1/E_2 = 100$, $\beta_2/\beta_1 = 100$, $K_1/K_2 = 10$).

thermal stress is smaller than that for the case where both the upper and lower surfaces are cooled by surrounding fluid at the same temperature, $T_u = T_l = -10°C$, shown in Figure 4.

Figure 7 shows the effects of the coefficient of thermal expansion ratio, β_2/β_1, on the normalized thermal stress distribution, σ_y, at the interface for the case where $T_u = T_l = T_0 = -10°C$ and the dimensionless time $F_r = 0.5$. From the figure, the compressive thermal stress increases steeply near the ends of the interface as β_2/β_1 increases.

Figure 8 shows the effects of the Young's modulus ratio, E_1/E_2, on the normalized thermal stress distribution, σ_y, at the interface for the case where $T_u = T_l = T_0 = -10°C$ and dimensionless time $F_r = 0.5$. Similarly to Figure 7, the compressive thermal stress increases steeply near the ends of the interface as E_1/E_2 increases.

4.2. Experimental Results

Figures 9 and 10 show examples of isochromatic fringe patterns generated on the epoxy resin plate modelled as an adhesive in the joint.

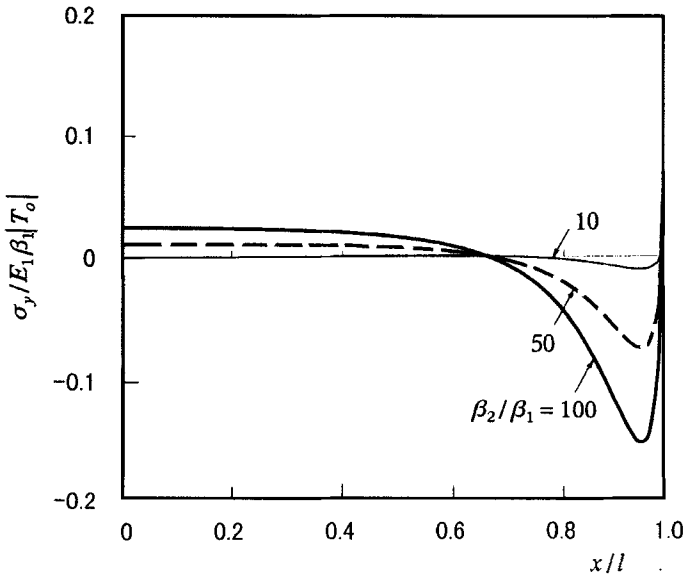

FIGURE 7 Effect of coefficient of thermal expansion ratio, β_2/β_1, on the thermal stress distributions at the interface ($T_u = T_l = -10°C$, $F_r = 0.5$, $h_1/h_2 = 2$, $E_1/E_2 = 100$, $K_1/K_2 = 10$).

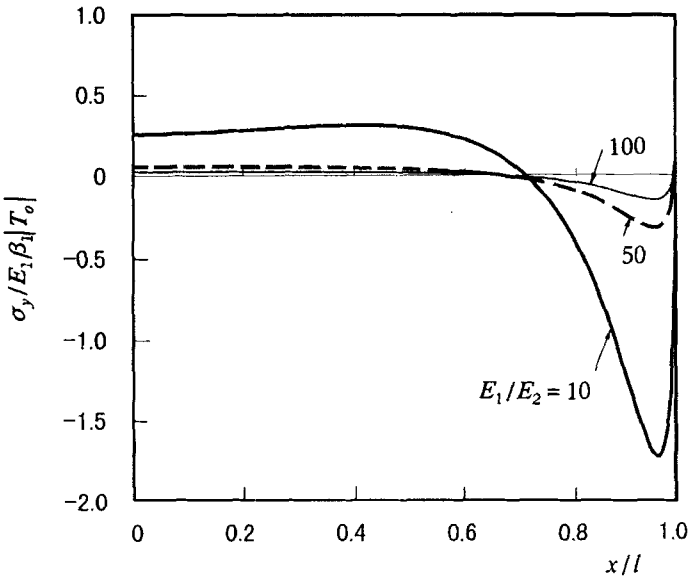

FIGURE 8 Effect of Young's modulus ratio E_1/E_2 on the thermal stress distributions at the interface ($T_u = T_l = -10°C$, $F_r = 0.5$, $h_1/h_2 = 2$, $\beta_2/\beta_1 = 100$, $K_1/K_2 = 10$).

Because of the symmetry with respect to the y axis, the fringe patterns on a half, the left-hand side, of the epoxy plate are shown in the figures.

The numerical results of the principal stress difference which coincides with the isochromatic fringe in principle are also shown for a half, the right-hand side, of the epoxy plate. Numbers shown in the numerical results indicate the orders of isochromatic lines. In these figures, T_u and T_l were denoted as the temperature difference between cooled water or a room temperature and a curing temperature (30°C) of the joint. In the numerical calculations, we used the heat transfer coefficients, α, of 3×10^{-3} W/(mm^{2}K) and 3×10^{-5} W/(mm^{2}K) when the upper and lower surfaces of the joint were cooled by surrounding water at 0°C and by air at 30°C, respectively. For easy comparison of these two results, the dimensionless time is taken as $F_r = a_2 t/h_0^2$ using the thermal diffusivity of the epoxy plate, $a_2 (= 0.14\,\text{mm}^2/\text{s})$.

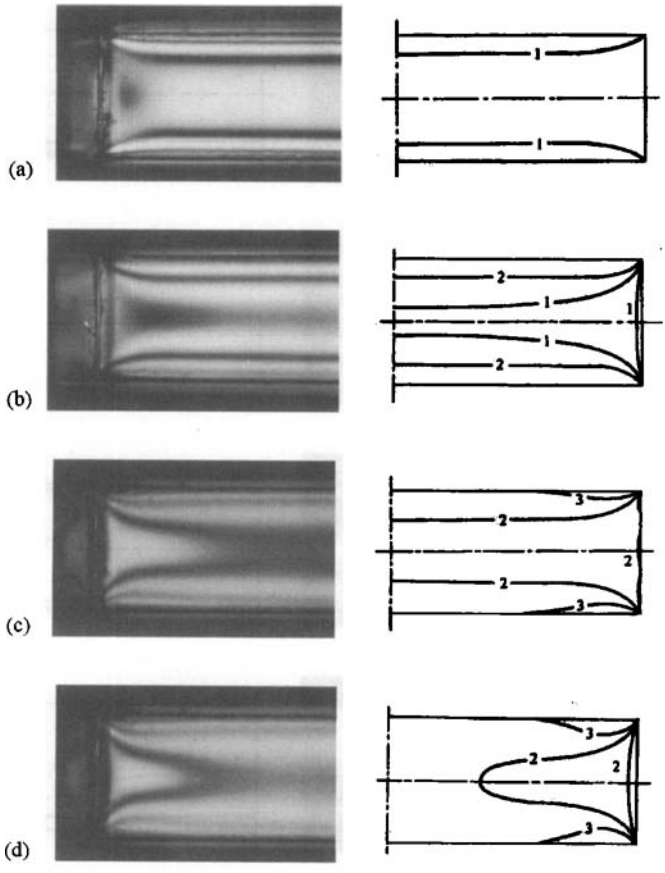

FIGURE 9 Photoelastic experimental results and comparison with the numerical results. (Steel adherends, $T_u = T_l = -30°C$, $E_1/E_2 = 60.6$, $\beta_2/\beta_1 = 5.45$, $2h_1 = 2h_3 = 10\,mm$, $2h_2 = 20\,mm$, $2l = 80\,mm$). (a) Photograph at $F_r = 0.02$, Numerically-obtained isochromatic pattern; (b) at $F_r = 0.10$; (c) at $F_r = 0.20$; (d) at $F_r = 0.80$.

Figure 9 shows the fringe pattern variations with the dimensionless time when both upper and lower surfaces of the joint were surrounded with cooled water of 0°C ($T_u = T_l = -30°C$). Both adherends of the joint were made of steel. Figure 10 is the case where the lower surface of the joint was surrounded with cooled water of 0°C, while the upper

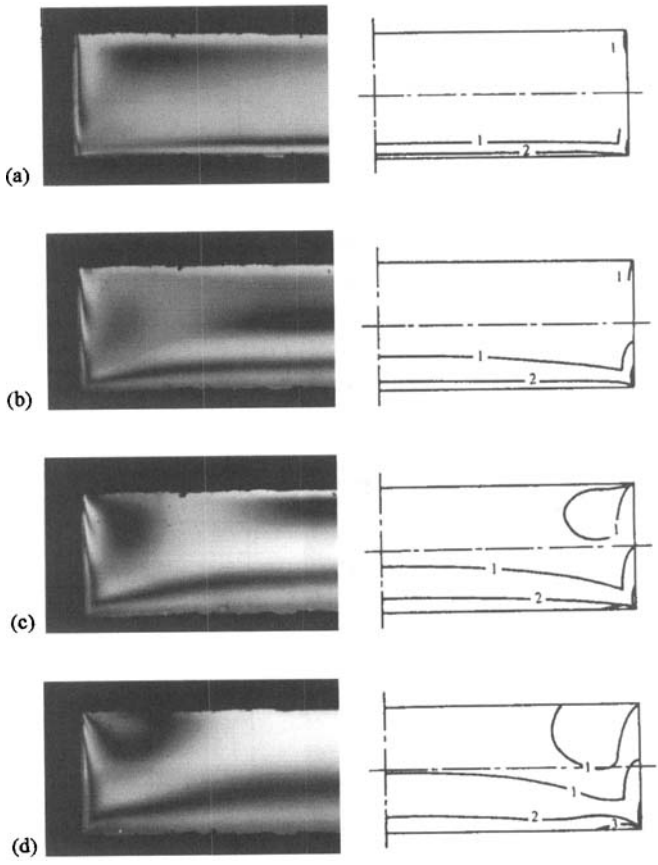

FIGURE 10 Photoelastic experimental results and comparison with the numerical results. (Copper adherends, $T_u = 0°C$, $T_l = -30°C$, $E_1/E_2 = 36.8$, $\beta_2/\beta_1 = 3.64$, $2h_1 = 2h_3 = 10\,mm$, $2h_2 = 20\,mm$, $2l = 80\,mm$). (a) Photograph at $F_r = 0.02$, Numerically-obtained isochromatic pattern; (b) at $F_r = 0.10$; (c) at $F_r = 0.20$; (d) at $F_r = 0.80$.

surface was surrounded with air at 30°C, ($T_u = 0°C$, $T_l = -30°C$). Both adherends were made of copper. From Figures 9 and 10, it is seen that the thermal stress concentration occurs near the ends of the interface and it increases with the passage of time; moreover, the numerical results obtained by the present transient thermal stress analysis are consistent with the experimental ones in each case.

5. CONCLUSIONS

The study deals with the transient thermal stress analysis in an adhesive butt joint when both the upper and lower surfaces of the joint are suddenly exposed to a surrounding fluid of constant temperature. An epoxy resin plate was used to model the adhesive and the thermal stress distribution in the epoxy plate was measured by photoelastic experiments and the experimental results were compared with the analytical ones. The results obtained are as follows:

(1) A method to analyze the transient thermal stress distribution in an adhesive butt joint when both the upper and lower surfaces of the joint are subjected to temperature change by a surrounding fluid is demonstrated by using the two-dimensional theory of elasticity.
(2) The effects of the coefficient of thermal expansion and Young's modulus ratios between the adherend and the adhesive on the transient thermal stress distributions at the interface are clarified numerically.
(3) Photoelastic experiments were carried out in order to confirm the transient thermal stress analysis. The experimental results were consistent with the numerical ones.

References

[1] Suhir, E., "Approximate Evaluation of the Elastic Thermal Stresses in a Thin Film Fabricated on a Very Thick Circular Substrate", *ASME J. Electronic Packaging* **116**, 171–176 (1994).
[2] Yin, Wan-Lee, "Interfacial Thermal Stresses in Layered Structures: The Stepped Edge Problem", *J. of Electronic Packaging* **117**, 153–158 (1995).
[3] Nakano, Y., Sawa, T. and Nakagawa, F., "Two-dimensional Thermal Stress Analysis of Butt Adhesive Joint", *JSME Intl. J. Ser. I* **35**(2), 145–151 (1992).
[4] Tanigawa, Y., Murakami, H. and Ootao, Y., "Transient Thermal Stress Analysis of a Laminated Composite Beam", *J. Thermal Stresses* **12**, 25–39 (1989).
[5] King, D. and Bell, J. P., "Thermal Shock Failure in Thick Epoxy Coatings", *J. Adhesion* **26**, 37–58 (1988).
[6] Kokini, K. and Smith, C. C., "Interfacial Transient Thermal Fracture of Adhesively Bonded Dissimilar Materials", *Exper. Mechanics* **29**, 312–317 (1989).
[7] Carslaw, H. S. and Jaeger, J. C., *Conduction of Heat in Solids* (Oxford University Press, Oxford, 1959).